Nuclear Thermal Propulsion Turbomachinery Modeling

Dennis Nikitaev, Corey D. Smith, and Kelsa Palomares

Advanced Projects Huntsville, Analytical Mechanics Associates, Huntsville, AL, 35806

Primary Author Contact Information: 702-287-6852, dennis.d.nikitaev@ama-inc.com

DOI: ####

The Nuclear Space Systems Analysis and Modeling (NSSAM) software which was previously developed by Analytical Mechanical Associates had the turbomachinery components upgraded. Instead of using a performance curve based on historical data, the turbomachinery parameters, including the shaft speed and component diameters, are calculated based on the required performance specifications. Performance maps are also shown to inform the user on various operating regimes of which the components are capable. Furthermore, these components could also operate at various conditions within their operating limits to allow for various thrust classes and transient analysis should these become options in NSSAM in the future.

I. INTRODUCTION

Nuclear Thermal Propulsion (NTP) is an in-space propulsion method which underwent significant development in the United States 1950s through the early 1970s during the Project Rover and Nuclear Engine for Rocket Vehicle Application (NERVA) programs. The goal of these two programs was to create a propulsion system capable of transporting humans to Mars and provide a reusable lunar shuttle. Unlike chemical propulsion, NTP does not depend on combustion of an oxidizer and fuel to produce thrust; instead, a propellant is pumped into a nuclear reactor and heated to high temperatures before being expelled through a nozzle. Essentially, the NTP-based engine is a monopropellant system[1]. In the early 1970s, the NERVA program was cancelled in favor of developing a reusable vehicle for Low Earth Orbit access called the Space Shuttle. Many studies and some development programs have been completed since this program, but none have reached the development status demonstrated in Rover/NERVA. In recent years, there has been renewed interest in development of NTP systems for crewed space exploration. Therefore, both government, academia, and industry have been developing both modern hardware and modeling approaches to bolster NTP development. One such model currently under development by Analytical Mechanics Associates (AMA) is the Nuclear Space System Analysis and Modeling (NSSAM) software which models the NTP system as an integrated reactor-engine system.

Current efforts are focused on developing an expander cycle NTP engine where no flow is bled to power the turbomachinery, thus, resulting in a more efficient system. Fig. 1 shows an expander cycle NTP engine schematic along with the state points of interest. The flow enters the pumps at State 1 and its pressure is raised at State 2 to accommodate all pressure losses and still provide enough pressure to the chamber at State 14. At State 3, the flow splits to provide regenerative cooling to the nozzle and the moderator elements to keep materials within their operating temperature. The valve prior to State 4 is a mass flow rate regulator valve which adjusts the amount of flow that goes to the nozzle at State 4 and to the moderator elements at State 7. The flow exits the nozzle at State 5 and enters the control drums and reflector to provide cooling to these elements as well. The flows that cool the moderator elements and control drums/reflector exit the reactor at States 8 and 6, respectively, and mix at State 9. Since the considered working fluid for NTP is usually hydrogen to provide high specific impulse, the phase of hydrogen at the considered conditions is supercritical. Since supercritical fluids have no surface tension and the flow rates are high to produce turbulent conditions, the mixing is assumed to be instantaneous and complete at State 9. At State 10, a portion of the flow from State 9 enters the turbine to provide the work required to drive the pump and exits the turbine at State 11. The valve below the turbine is the Turbine Bypass Valve (TBV) and controls the amount of flow enters the turbine to throttle the pumps. At State 12, the TBV and Turbine discharge flows mix and at State 13, pre-reactor conditions are obtained. The flow is heated between State 13 and 14 with State 14, as mentioned previously, is the chamber. The flow is expelled out through the nozzle to provide thrust and State 15 is the nozzle discharge.

NSSAM enables accessible and customized systems engineering analyses of the design space of space reactor systems. The code suite is built in an object-oriented Python environment due to its capability to ensure high-cohesion and low-coupling for scalability and extensibility. Python allows for NSSAM to automate complex calculations and seamlessly pass information between codes, without the user needing detailed knowledge of reactor physics or thermal hydraulic systems. This includes

writing input files, calling and running external software (such as Monte Carlo based reactor physics codes), and extracting meaningful outputs from external software output files. The NSSAM software architecture enables extensibility across the different space reactor systems and design variants of each of the system components via a model-view-controller pattern, thus enabling the user to operate NSSAM under various use cases. A more detailed description of NSSAM was provided in previous work[2]. Although NSSAM has the capability for detailed and scalable reactor modelling, a significant limitation of previous versions was the turbomachinery models which used curve fits based on historical data for predicting pump performance, thereby limiting the operational regime and thrust levels that could be analyzed. Since modularity is a key component of NSSAM, a higher fidelity turbomachinery model was desired to be implemented to allow the user to analyze multiple variants of reactor-engine combinations and performance parameters (thrust, specific impulse, etc.).

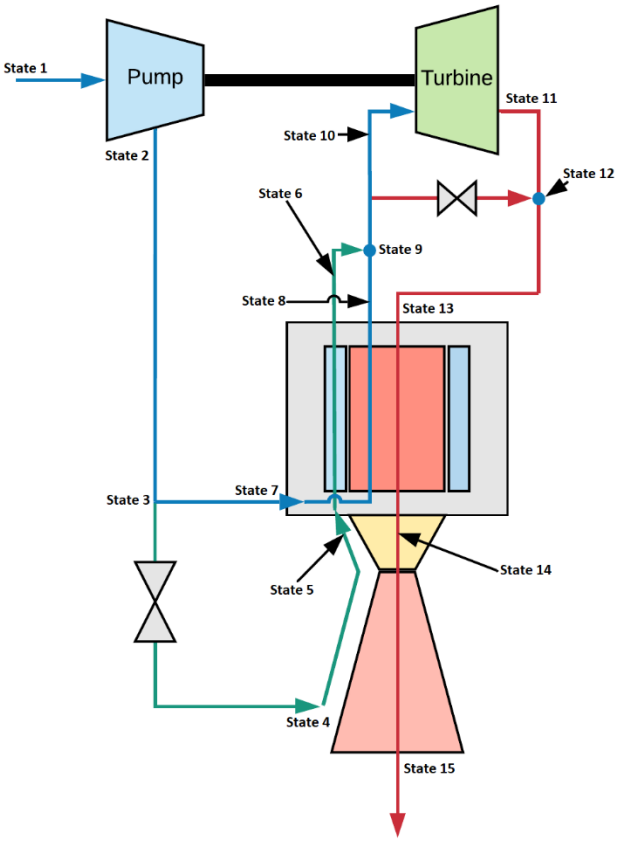

Fig. 1. NTP Engine Schematic[2]

II. TURBOMACHINERY ANALYTICAL FORMULATIONS

II.A. Pumps

The purpose of the pump is to supply the pressure required to overcome frictional and acceleration pressure losses through all channels throughout the engine, provide the pressure required to drive the turbines, and provide the required pressure inside the chamber for the nozzle to produce thrust. Although pressure fed systems are technically possible from the engine standpoint, they will be infeasible from the vehicle standpoint as the propellant tanks will require high mass to contain the high-pressure propellant[3]. Other studies were done on turbomachinery systems for NTP engine models, however, their hydrogen pump parameters are proprietary[4–6]. Prior work[5] performed validation of the methodology described in this paper for both pumps and turbines for hydrogen-based NTP engines.

The pressure requirements start at the chamber and are determined upstream through the flow up to the pumps where the maximum system pressure occurs. The difference between the pump inlet P_{in} and maximum system pressure or pump discharge pressure P_{out} is characterized by the by the pump pressure head H_p for which the expression is shown in Eq. (1) where ρ is the fluid density and g_0 is the reference acceleration due to gravity on Earth at sea level. Pumps could also be cascaded together to avoid cavitation at pump inlets and reduce the required pump pressure head across the individual pumps. The number of pumps used in NSSAM can vary depending on the required maximum system pressure. The work that the pump produces W_p is directly related to the volumetric flow rate through the pump $\dot{\forall}_p$, the fluid density ρ, and the pump pressure head H_p as shown in Eq. (2). This can further be related to the available and exit pressure as well as the fluid enthalpy. The type of pump that is used is specified by the pump specific speed n_{s_p} and the pump types according to this parameter are shown in Fig. 2. This specific speed parameter can be used to determine the shaft speed of the pump ω by using Eq. (3) (Refs. 3–5).

$$H_p = \frac{P_{out} - P_{in}}{g_0 \rho} \tag{1}$$

$$\dot{W}_p = \rho g_0 \dot{\forall}_p H_p = \frac{\dot{m}_p (P_{out} - P_{in})}{\rho} \tag{2}$$

$$\omega = \frac{n_{s_p} (g_0 H_p)^{3/4}}{\sqrt{\dot{\forall}_p}} = \frac{n_{s_p} (P_{out} - P_{in})^{3/4}}{\rho^{1/4} \sqrt{\dot{m}_p}} \tag{3}$$

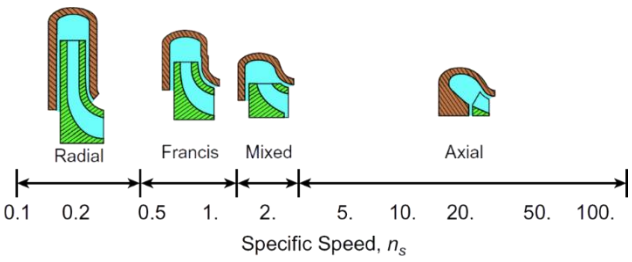

Fig. 2. Types of Pumps According to the Specific Speed[3]

An important pump characteristic is the pump efficiency η_p, which according to Fig. 3, is a function of both the pump specific speed n_{s_p} and pump specific diameter d_{s_p}. The pump specific diameter is a parameter that depends on the physical diameter D_p of the pump for which the expression is shown in Eq. (4). Once both the work done by the pump W_p and the efficiency of the pump have been determined, the work required to drive the pump W_{shaft} can be found by using Eq. (5). Furthermore, the temperature rise through the pump can also be determined by implementing the First Law of Thermodynamics for an open system, assuming steady state, to find the enthalpy of the fluid coming out of the pump as shown in Eq. (6). The $\dot{Q}_{in}$ is the heat that goes into the pump from external means such as the radiative heat absorbed from the reactor. This is mostly a third order effect which could be calculated based on either a simple approach from historical data or directly calculating the radiative heat deposition on the outside shell of the pump. The outlet enthalpy value along with the resulting pressure can be used in a programmatic fluid property library such as CoolProp[6] or on a *P-h* diagram for the specific fluid to find the fluid outlet temperature[3–5].

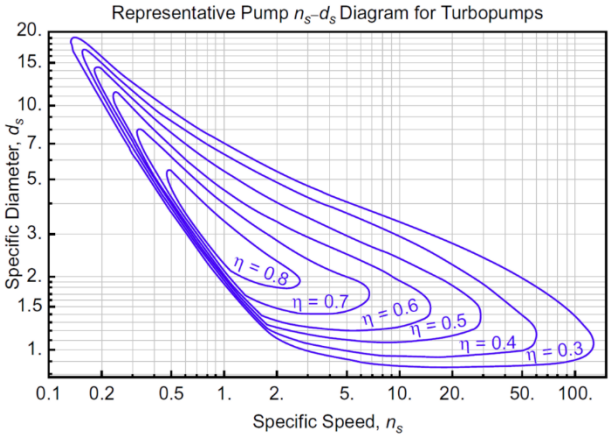

Fig. 3. Pump Efficiency[3]

$$d_{s_p} = \frac{D_p(g_0 H_p)^{1/4}}{\sqrt{\dot{\forall}_p}} = \frac{D_p[\rho(P_{out}-P_{in})]^{1/4}}{\sqrt{\dot{m}_p}} \quad (4)$$

$$W_{shaft} = \frac{W_p}{\eta_p} \quad (5)$$

$$h_{out} = h_{in} + \frac{\dot{Q}_{in}-\dot{W}_p}{\dot{m}_p} \quad (6)$$

Cavitation is an important physical phenomenon that needs to be considered since prolonged occurrence can damage the pump. When the pump pressurizes the fluid, the pressure is reduced at the pump inlet depending on the pump speed. When the pressure is reduced below the fluid's vapor pressure P_v evaluated at the inlet temperature, cavitation will occur. Therefore, there exists a minimum inlet pressure $P_{in_{min}}$ that is required to prevent cavitation and is defined by Eq. (7). In most cases, $P_{in_{min}}$ is an over-estimate and the α term in Eq. (7) represents the margin by which P_{in} can be below $P_{in_{min}}$ which is usually set to 10% (Ref. 7). The other term that appears in Eq. (7) is σ which is called the Thoma parameter and can be found by determining the suction-specific speed s_s shown in Eq. (8) and using the empirical correlation to the pump specific speed n_{s_p} shown in Fig. 4 (Ref. 3–5).

$$P_{in_{min}} = (1-\alpha)\sigma(P_{out}-P_{in}) + P_v \quad (7)$$

$$s_s = \frac{\omega\sqrt{\dot{\forall}_p}}{\left(\frac{P_{in}-P_v}{\rho}\right)^{3/4}} = \frac{\omega\rho^{1/4}\sqrt{\dot{m}_p}}{(P_{in}-P_v)^{3/4}} \quad (8)$$

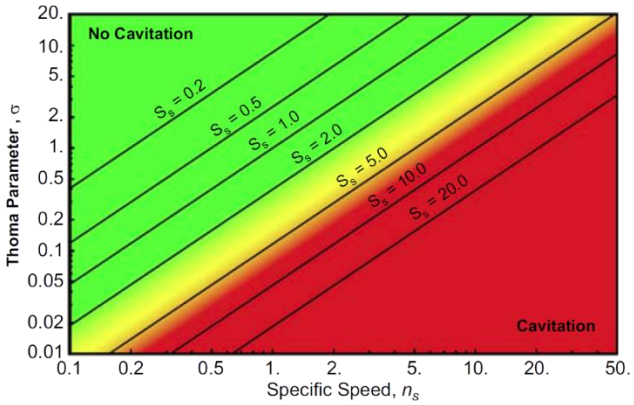

Fig. 4. Correlation of Cavitation with Pump Suction Specific Speed[3]

II.B. Turbines

The turbines are tasked with providing the work that the pumps require via shaft, therefore $\dot{W}_{turb} = \dot{W}_{pump}$. Just as with pumps, the specific speed of the turbine n_{s_t} determines the turbine type. Unlike the pumps which are tasked with pressurizing a liquid, turbines deal with gases which have the behavior of compressible fluids, therefore the turbine head H_t is expressed through the fluid enthalpies instead of the pressures as shown in Eq. (9). Fig. 5 shows the various turbine types with respect to the n_{s_t}.

$$n_{s_t} = \frac{\omega\sqrt{\dot{\forall}_t}}{(g_0 H_t)^{3/4}} = \frac{\omega\sqrt{\dot{m}_t}}{\sqrt{\rho}(h_{in}-h_{out})^{3/4}} \quad (9)$$

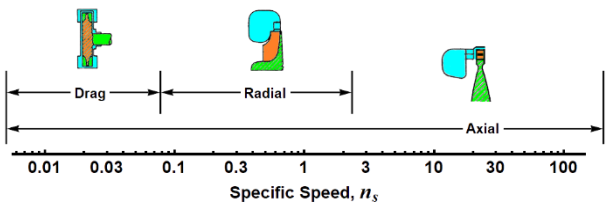

Fig. 5. Types of Turbines According to the Specific Speed[3]

A similarity between the turbine and pump calculations is the specific diameter d_s which is based on the physical diameter D. Just like in the turbine specific speed expression, the pressure head is replaced by the enthalpy change as shown in Eq. (10). Together, n_{s_t} and d_{s_t} determine the efficiency of the turbine η_t as shown in Fig. 6. This contour plot can be transferred into a table and η_t looked up in terms of n_{s_t} and d_{s_t} just like in the case of the pump analysis.

$$d_{s_t} = \frac{D_t(g_0 H_t)^{1/4}}{\sqrt{\dot{\forall}_t}} = \frac{D_t\sqrt{\rho}(h_{in}-h_{out})^{1/4}}{\sqrt{\dot{m}_t}} \qquad (10)$$

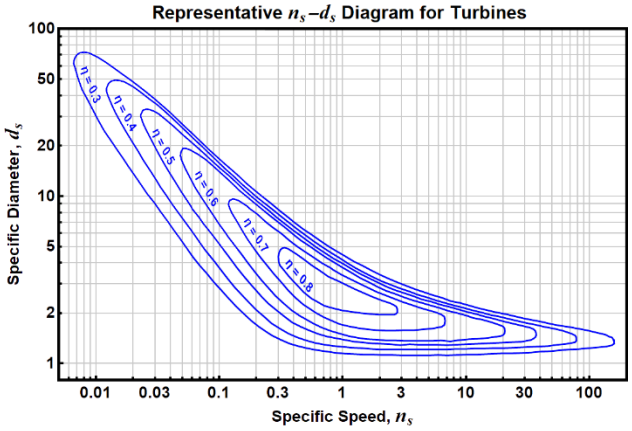

Fig. 6. Representative $n_{s_t} - d_{s_t}$ Diagram for Turbines[3]

Since turbines can be throttled by controlling the mass flow rate, it is important to now calculate the turbine mass flow rate $\dot{m}_t$ to produce a required amount of work. Given the turbine stagnation inlet temperature $T_{0_{in}}$ and pressure $P_{0_{in}}$ calculated from the moderator and reflector exit channels, the work required $\dot{W}_{shaft}$, the shaft speed ω, external heat $\dot{Q}_{in}$, n_{s_t}, and turbine physical diameter D_t, $\dot{m}_t$ is found by setting the outlet enthalpy h_{out} from the First Law of Thermodynamics equal to the outlet enthalpy from the turbine specific speed equation (Eq. (11)). The inlet enthalpies h_{in} cancel and solving for $\dot{m}_t$ yields Eq. (11).

$$\dot{m}_t = \left(\dot{W}_{shaft} - \dot{Q}_{in}\right)^{3/5}\left(\frac{n_{s_t}\sqrt{\rho}}{\omega}\right)^{4/5} \qquad (11)$$

An important parameter that determines turbine performance is the discharge pressure which can be used to find the pressure ratio of the turbine. Although the pressure ratio can be specified and the efficiency calculated from that pressure ratio, it is only valid for steady, non-transient analysis. Because the turbine inlet conditions and the work required will change during transient scenarios, it is important to determine the pressure ratio as a function of the turbine characteristics. This is done by finding the turbine efficiency η_t from n_{s_t} and d_{s_t}, as discussed previously. Since $\dot{m}_t$ is calculated by setting the outlet enthalpy h_{out} equal to the outlet enthalpy from the turbine specific speed equation (Eq. (9)), all the components that are necessary for determining h_{out} are in place and either the First Law of Thermodynamics or the turbine specific speed equation (Eq. (9)) could be used to find it. Furthermore, since the turbine inlet temperature and pressure are known, the inlet enthalpy h_{in} is also known.

The turbine efficiency along with the inlet and outlet enthalpies can be used to determine the isentropic outlet enthalpy h_{out_s} by using the thermodynamic efficiency equation for turbines as shown in Eq. (12). To find any thermodynamic quantity, only two quantities must be known[8]. Since both the inlet conditions and h_{out_s} are known, the outlet conditions are defined by linking the inlet entropy s_{in} to h_{out_s} and finding the outlet stagnation pressure $P_{0_{out}}$ from fluid property look-up tables such as CoolProp[6]. Using both h_{out} and $P_{0_{out}}$, the outlet stagnation temperature $T_{0_{out}}$ and other thermodynamic properties can be determined.

$$\eta_t = \frac{h_{in}-h_{out}}{h_{in}-h_{out_s}} \rightarrow h_{out_s} = h_{in} - \frac{h_{in}-h_{out}}{\eta_t} \qquad (12)$$

III. DETERMINING TURBOMACHINERY PARAMETERS

To determine the turbomachinery parameters, the program must first evaluate the reactor performance and required inlet pressures for the various reactor channels. The user inputs the reactor parameters such as fuel geometry specifications, moderator type (block or tie-tube), reflector geometries, and channel geometries. The required turbomachinery performance parameters are evaluated after the reactor converges to a user specified chamber temperature and pressure. Once convergence is achieved, the required reactor flow inlet conditions and the flow outlet conditions of the pre-fuel elements for the turbine inlet are known, assuming an expander cycle. This means that given specified tank conditions, the ΔP that the pump system must produce is known. NSSAM provides the option to either manually specify the physical diameter and specific speed of the pump or automatically determine these parameters given a maximum shaft velocity and pump material by finding the parameter pair that maximizes the pump efficiency.

The number of pumps and turbines should also be specified as these affect the engine mass and performance of these systems. More pumps result in lower chances of cavitation since the total ΔP load is split between each pump and according to Eq. (7), this has a direct impact on the minimum inlet pressure to prevent cavitation. More turbines usually result in lower required mass flow rate as the total work that must be produced is shared across all the turbine disks. As the workload decreases per disk, so does

the required mass flow rate according to Eq. (11). However, increasing the number of each component will result in an increase of the engine mass.

Should the user ask NSSAM to automatically find the pump parameters, it will show the pump efficiency contour map as a function of the pump diameter and shaft velocity. This will show the justification of why the pump parameters were selected as well as an infeasibility range where the pump diameter is too high to support the rotational velocity. The maximum diameter is based on the yield stress σ_y of the material selected, a rotor shape factor S which is assumed to be 0.3 as a conservative estimate, the rotor density ρ_r, and an assumed factor of safety ξ of 2 as shown in Eq. (13) (Ref. 3). The currently supported pump and turbine materials are shown in Table I with the difference in yield stresses reflecting the operating regime assuming cryogenic fluids inside the pump. Future work will expand upon this database and include curve fits with respect to temperature for each material.

$$D_{max} = \sqrt{\frac{4\sigma_y}{\xi S \rho_r \omega^2}} \tag{13}$$

TABLE I. NSSAM Material Property Database

Material	σ_y for Pump (MPa)	σ_y for Turbine (MPa)	Density (kg/m^3)
Stainless Steel	344	207	8060
Aluminum	372	276	2700
Brass	300	140	8730
Bronze	372	125	8900
Inconel	1241	550	8192
Titanium	1240	240	4500

An example of the automatic pump determination is shown in Fig. 7 for a pump made of titanium. The input conditions used as well as the resulting pump parameters are shown in Table II. It is important to see that although the shaft rotational velocity is quite high of around 87,500 RPM, it is still below the red area which indicates the pump diameter limit at the respective speed. It should further be noticed that the design point is located at the area of maximum efficiency which confirms that the code properly selected the most efficiency pump given the operating conditions, requirements, and constraints as shown in Table II.

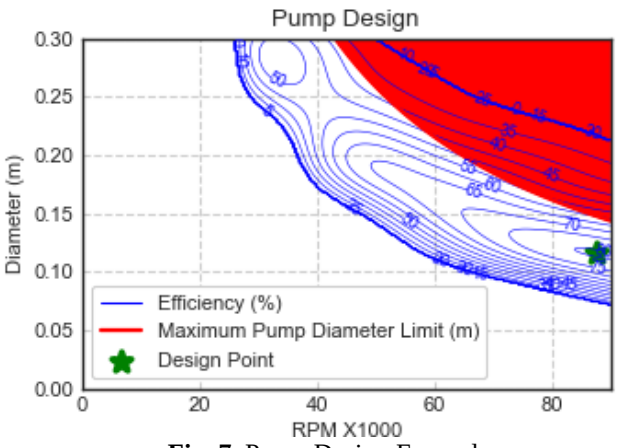

Fig. 7. Pump Design Example

TABLE II. Example Pump Design Specifications

Parameter	Value	Units
Number of Pumps	2	-
Pump Material	Titanium	-
Mass Flow rate	12.6	kg/s
Inlet Temperature	20	K
Inlet Pressure	355	kPa
Maximum Considered Speed	90,000	RPM
Design Speed	87,524	RPM
Design Diameter	0.1164	m
Design Efficiency	80.31	%

Based on these pump parameters, a pump performance map can be generated for the specific pump designed. An example based on the pump design in Fig. 7 is shown in Fig. 8. Here, the performance parameters are shown as dependent functions of the mass flow rate and the required ΔP. In Fig. 8, like in Fig. 7, the blue contours represent the efficiency. Other contours are present in Fig. 8 with black representing the rotational velocity and red representing the work required by the pump to operate at that state. The green star shows the design operation regime from the efficiency-optimization sequence. Here, it is clearly seen that the program chose the highest efficiency in the specified rotational velocity range. Although a rotational velocity of 87,500 RPM may seem as high, the diameter is only 11.64 cm, which leads to acceptable stress levels according to the design point being below the maximum diameter limit as was shown in Fig. 7.

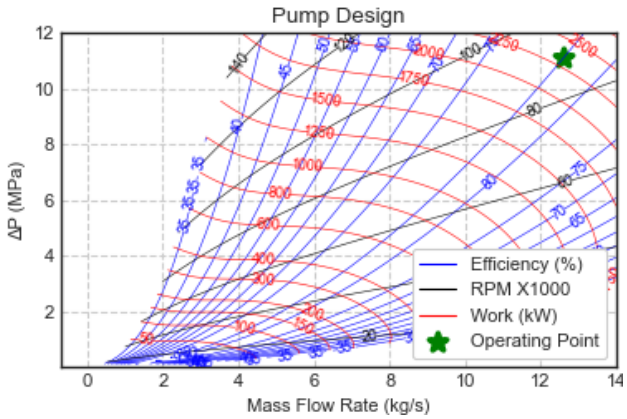

Fig. 8. Pump Performance Map Example

The turbine is designed based on the work required by the pump, the pump rotational velocity assuming that both the pump(s) and turbine(s) are on the same shaft, and the turbine pressure ratio specified by the user. NSSAM converges based on a set turbine pressure ratio to reach a desired reactor inlet pressure, so the turbine efficiency is the only other performance parameter that can be varied by manipulating the turbine diameter and specific speed. Like the pump, a maximum turbine diameter is found by using Eq. (13). The user can select the criteria for convergence of the turbine by choosing either the pressure ratio or the required flow rate fraction through the turbine bypass valve. The bypass valve option will lock in a flow rate through the turbine and determine a set of parameters that satisfy this flow rate. The efficiency will be maximized in either case and is achieved by utilizing a least squares optimization technique. Once the turbine parameters have been found, a turbine performance map is plotted as shown in the example map in Fig. 9 which was calculated to match the pump design shown in Fig. 7. The performance parameters are depicted as dependent functions of the pump work required and the rotational velocity of the shaft. This allows the pump to guide the performance regime of the turbine to produce the required ΔP as dictated by the reactor analysis codes. Like in Fig. 7 and Fig. 8, the design operation point is indicated by the green star, and the blue contours represent the turbine efficiency. The other parameters shown are the required mass flow rate through the turbine in black and the resulting turbine pressure ratio in red. Although NSSAM is not currently outfitted with a transient engine analysis capability, the key takeaway of the performance maps shown in Fig. 8 and Fig. 9 is that the user can map out the turbomachinery transient performance and gain insight into the sustainable throttleability of the engine before the turbine bootstrapper must take effect. Furthermore, if another program is developed that caters specifically to transient engine analysis, the performance parameters generated by NSSAM could serve as inputs for the model given the same turbomachinery. The development of a transient analysis code is left for future work.

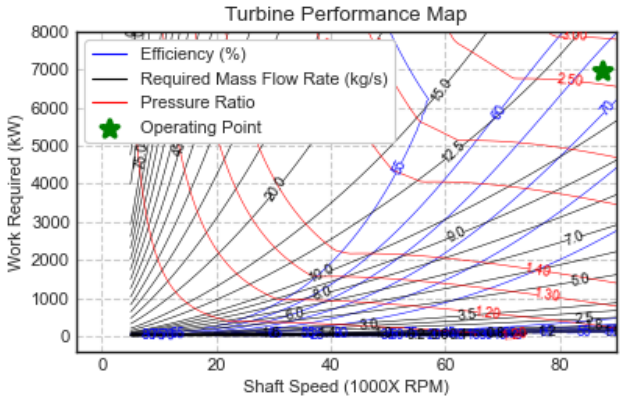

Fig. 9. Turbine Performance Map Example

IV. CONCLUSIONS

The NSSAM software has been designed by AMA to enable assessment of the reactor and engine trade space by leveraging a scalable and extensible software architecture that automates system-level analyses. This capability has been expanded to automate the engine turbomachinery analysis for identifying fluid temperature and pressure at key state points of the reactor-engine power balance. This new process allows NSSAM to flexibly calculate the turbomachinery parameters through efficiency optimization or manually input pump and turbine characteristic parameters. It was important to consider the link between the isentropic efficiency and the turbine efficiency from the contour efficiency map as this relation locked the thermodynamics with the turbine parameters. From there, variable turbine pressure ratios were able to be determined based on the pump work required and shaft speed. Furthermore, approaching the turbomachinery coding from a modular standpoint which considered the ability to change number of turbomachinery stages seamlessly and off nominal operation proved to be very beneficial when different operating regimes could be considered. The outputs of NSSAM will provide insight into transient engine performance by displaying performance maps of the turbomachinery evaluated. Future work will include a more extensive and detailed pump and turbine material property library and the creation of a transient analysis engine code.

ACKNOWLEDGMENTS

This work was supported by NASA's Space Technology Mission Directorate (STMD) through the Space Nuclear Propulsion (SNP) project. This work was funded under Contract No. 80LARC17C0003.

REFERENCES

[1] Robbins, W. H., and Finger, H. B. *An Historical Perspective of the NERVA Nuclear Rocket Engine*

Technology Program. Publication NASA-CR-187154. Analytical Engineering Corporation, 1991.

[2] Palomares, K., Harnack, C., Smith, C., Herner, R., Machemer, W., Rawlins, S., Grella, E., and Boylston, A. Nuclear Space System Analysis and Modelling (NSSAM): A Software Tool to Efficiently Analyze the Design Space of Space Reactor Systems. Presented at the Nuclear and Emerging Technologies for Space, Virtual Event, 2021.

[3] Chakroborty, Shyama and Bauer, Thomas P. Using Pressure-Fed Propulsion Technology to Lower Space Transportation Costs. Presented at the 40th AIAA/ASME/SAE/ASEE Joint Propulsion Conference and Exhibit, Fort Lauderdale, FL, 2004.

[4] Joyner, C. R., Eades, M., Horton, J., Jennings, T., Kokan, T., Levack, D. J. H., Muzek, B. J., and Reynolds, C. B. "LEU NTP Engine System Trades and Mission Options." *Nuclear Technology*, Vol. 206, No. 8, 2020, pp. 1140–1154. https://doi.org/10.1080/00295450.2019.1706982.

[5] Nikitaev, D., and Thomas, L. D. "Seeded Hydrogen in Nuclear Thermal Propulsion Engines." *Journal of Spacecraft and Rockets*, Vol. 57, No. 5, 2020, pp. 907–917. https://doi.org/10.2514/1.A34711.

[6] Nikitaev, D., and Thomas, D. L. "Alternative Propellant Nuclear Thermal Propulsion Engine Architectures." *Journal of Spacecraft and Rockets*, 2022, pp. 1–11. https://doi.org/10.2514/1.A35289.

[7] Emrich, W. Jr. *Principles of Nuclear Rocket Propulsion*. Butterworth-Heinemann, Kidlington, Oxford, United Kingdom, 2016.

[8] Balje´, O. E. "A Study on Design Criteria and Matching of Turbomachines: Part A—Similarity Relations and Design Criteria of Turbines." *Journal of Engineering for Power*, Vol. 84, No. 1, 1962, pp. 83–102. https://doi.org/10.1115/1.3673386.

[9] Balje´, O. E. "A Study on Design Criteria and Matching of Turbomachines: Part B—Compressor and Pump Performance and Matching of Turbocomponents." *Journal of Engineering for Power*, Vol. 84, No. 1, 1962, pp. 103–114. https://doi.org/10.1115/1.3673350.

[10] Bell, I. H., Wronski, J., Quoilin, S., and Lemort, V. "Pure and Psuedo-Pure Fluid Thermophysical Property Evaluation and the Open-Source Thermophysical Property Library CoolProp." *Industrial & Engineering Chemistry Research*, Vol. 53, 2014, pp. 2498–2508. https://doi.org/10.1021/ie4033999.

[11] Knuth, W. UAH Technical Faculty. Jun 06, 2019.

[12] Moran, Michael J., Shapiro, Howard N., Boettner, Daisie D., and Bailey, Margaret B. *Fundamentals of Engineering Thermodynamics*. John Wiley & Sons, Inc, 2014.